

Received: 2017.09.21

Accepted: 2018.03.11

Published: 2018.07.03

# Pathogenesis of Abnormal Hepatic Lipid Metabolism Induced by Chronic Intermittent Hypoxia in Rats and the Therapeutic Effect of N-Acetylcysteine

Authors' Contribution:  
Study Design A  
Data Collection B  
Statistical Analysis C  
Data Interpretation D  
Manuscript Preparation E  
Literature Search F  
Funds Collection G

ABCDEFG 1,2,3

BDE 1,2

CEF 1,2

CF 1,2

CE 1,2

DE 1,2

ADEG 1,2

**Haipeng Wang**

**Yan Wang**

**Tongliang Xia**

**Yaxuan Liu**

**Ting Liu**

**Xiaoli Shi**

**Yanzhong Li**

1 Department of Otolaryngology Head and Neck Surgery, Qilu Hospital of Shandong University, Jinan, Shandong, P.R. China

2 Key Laboratory of Otorhinolaryngology of Health Ministry, Shandong University, Jinan, Shandong, P.R. China

3 Department of Otolaryngology Head and Neck Surgery, Zibo City Central Hospital, Zibo, Shandong, P.R. China

**Corresponding Author:** Yanzhong Li, e-mail: liyanzhong@sdu.edu.cn

**Source of support:** This work was supported by the National Natural Science Foundation of China (grant number 81170903 to Yanzhong Li)

**Background:** The pathogenesis of chronic intermittent hypoxia (CIH)-induced abnormal hepatic lipid metabolism in rats remains unclear. Here, we investigated the therapeutic effect of N-acetylcysteine (NAC) on abnormal hepatic lipid metabolism.

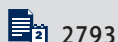
**Material/Methods:** Rats were subjected to hypoxia and NAC treatment, and evaluated in terms of hepatic lipid metabolism, hepatocyte ultrastructure, oxidative stress in hepatocytes, expression of nuclear factor-kappa B (NF- $\kappa$ B) and inflammatory cytokines (IL-1 $\beta$ , IL-6, and TNF $\alpha$ ), serum lipoprotein lipase (LPL) levels, and blood lipids (triglycerides and cholesterol).

**Results:** Compared to the normoxic control group, animals in the hypoxic model group showed significant body weight gain; abnormal hepatic lipid metabolism; lipid vacuolization; accumulation of lipid droplets; abundant autophagosomes and lysosomes; significant increases in oxidative stress, inflammation level, and blood lipid levels; and significantly reduced LPL levels. Compared to control animals, rats in the treatment group exhibited normal body weight gain, improved lipid metabolism, fewer lipid droplets, alleviated ultrastructural injuries, decreased oxidative stress and inflammation level, as well as elevated LPL and reduced blood lipid levels.

**Conclusions:** The harmful effects of CIH on rat liver are possibly associated with the reactive oxygen species (ROS)/NF- $\kappa$ B signaling pathway. NAC is capable of attenuating lipid metabolism alterations and abnormal body weight gain in the CIH rat model, via a possible mechanism related to inhibition of ROS/NF- $\kappa$ B signaling.

**MeSH Keywords:** **Acetylcysteine • Cell Hypoxia • Lipid Metabolism • Oxidative Stress**

**Full-text PDF:** <https://www.medscimonit.com/abstract/index/idArt/907228>



2793



2



4



25



## Background

Obstructive sleep apnea (OSA) affects multiple body systems. Its pathophysiological basis is chronic intermittent hypoxia (CIH)/reoxygenation. This leads to nocturnal hypoxemia and the generation of oxygen free radicals through ischemia-reperfusion injury, with the onset of both local and systemic inflammatory responses that cause liver, lung, and cardiovascular damage [1]. Clinical and basic studies have confirmed that severity of hypoxia in OSA patients is closely related to abnormal hepatic lipid metabolism, fatty liver formation, and elevated blood lipid levels [2–6]. Animal models have indicated that CIH can cause injury in multiple organs in rats, with different organs showing varying sensitivities to CIH [7]. In this study, we aimed to investigate the molecular and cellular effects of CIH on hepatic lipid metabolism in rats and its underlying pathogenesis. We also investigated its mechanism of action by drug intervention experiments to provide a theoretical basis for the clinical treatment and prevention of OSA syndrome.

## Material and Methods

### Materials and reagents

NAC (99.9% purity) and Oil Red “O” were obtained from Sigma-Aldrich Company (St. Louis, MO, USA). Optimum cutting temperature embedding medium and RIPA Lysis Buffer were obtained from Sakura Biological Technology Co., Ltd (USA). Dihydroethidium (DHE) fluorescence probe was obtained from Beyotime Institute of Biotechnology (Shanghai, China). Primary antibodies against  $\beta$ -actin, interleukin (IL)-1 $\beta$ , IL-6, tumor necrosis factor alpha (TNF $\alpha$ ), and nuclear factor-kappa B (NF- $\kappa$ B) p65 were obtained from Abcam (Cambridge, MA, USA). Trizol RNA reagent and the real-time PCR kit were obtained from TaKaRa Bio (Kyoto, Japan). Primers were obtained from RuiDi Biological Technology (Shanghai, China). Lipoprotein lipase (LPL) was obtained from R&D Systems (Minneapolis, MN, USA). Triglyceride (TG) and total cholesterol (TC) were obtained from Jiancheng Bioengineering Institute (Nanjing, Jiangsu, China).

### Animals and equipment

A total of 60 healthy, 8-week-old, male Wistar rats of clean grade were provided by the Laboratory Animal Center of Shandong University, China. The CIH chamber and high-purity nitrogen (99.999%) were supplied by the Key Laboratory of Otolaryngology of the Health Ministry, Shandong University. All experiments were approved by the Shandong University Animal Care Committee and conducted in accordance with rules set by the Chinese Council on Animal Care.

### Animal model

The 60 rats were randomly divided using a random number table into 4 groups with 15 rats each: normoxic control (CON), CIH model (CIH), CIH+0.9% NaCl model control (CIH+NS), and CIH+N-acetylcysteine treatment (CIH+NAC). The rats were exposed for 1 week to the same experimental conditions of 23°C, 50% humidity, and normal feeding. The hypoxia chamber was set to a low oxygen concentration of 5% for 40 s and a normoxic period of 40 s (both with a buffering period of 5 s) in a hypoxia-normoxia-hypoxia cycle for 8 h daily from 09:00 to 17:00 for 9 weeks [8]. Rats in groups CIH+NAC and CIH+NS were injected intraperitoneally with NAC+NS (20 mg/Kg/d, 1%) [9,10] and an equal volume of NS daily 15 min prior to hypoxic treatment for a total of 9 weeks. Their initial and final body weights (g) were recorded.

### Preparation of histological samples

For hematoxylin and eosin (HE) staining, paraffin-embedded liver specimens were prepared by sectioning the tissue into 4.5- $\mu$ m-thick sections. Sections were then dewaxed and hydrated prior to HE staining. Next, stained tissue sections were subjected to gradient dehydration, transparentizing, and mounting prior to observation by light microscopy.

For Oil Red “O” staining, rat livers were perfused by 0.9% NaCl, then excised and embedded in optimal-cutting-temperature compound, quick-frozen on dry ice, and stored at  $-80^{\circ}\text{C}$ . Frozen sections were then thawed at  $23\text{--}25^{\circ}\text{C}$  and hydrated. Oil Red “O” staining was performed for 10 min. Serial 12- $\mu$ m-thick sections were obtained by use of a sliding microtome (Leica CM1900, Nussloch, Germany) and mounting prior to light microscopy observation and quantification using Image-Pro Plus software (Media Cybernetics, Rockville, MD, USA).

For transmission electron microscopy (TEM), specimens were rinsed, fixed, dehydrated, infiltrated, and embedded, followed by ultrathin sectioning and electron microscopy staining prior to observation.

### Detection of ROS using DHE fluorescence

Frozen sections were thawed to room temperature for 30 min and then rinsed 3 times with phosphate-buffered saline (PBS) for 5 min each. Next, the sections were incubated with a DHE fluorescence probe at  $37^{\circ}\text{C}$  for 25 min and rinsed again with PBS prior to observation by fluorescence microscopy and quantification using Image-Pro Plus software.

**Table 1.** Sequences of primers used for real-time PCR.

Name	Forward primer (5'-3')	Reverse primer (5'-3')
NF-κB	TTCAACATGGCAGACGACGA	CCATCTGTTGACAGTGGTATATCTG
IL-1β	GGTCCTCTTTACCGGGCTC	GGACAACCAGGAGTCGTCTG
IL-6	CCAGTTGCCTTCTGGGACT	TTCTGACAGTGCATCATCGCT
TNFα	TGCAGCCTCCTAAAGTCTGTG	CTGTTCCGGGGAGAGGTAG
β-actin	CTGTGTGGATTGGTGGCTCT	CAGCTCAGTAACAGTCCGCC

### Immunohistochemical staining

Paraffin sections of liver specimens were deparaffinized, rehydrated, and unmasked, followed by rinsing with PBS and incubation at room temperature. Next, the sections were rinsed again and blocked with 10% normal goat serum at 37°C for 30 min, followed by overnight incubation at 4°C with the primary antibody (or PBS in the CON group). Sections were then thawed at 37°C, rinsed, and dried prior to incubation at 37°C for 20 min with the secondary antibody added dropwise. Next, sections were rinsed again and stained with freshly prepared 3,3-diaminobenzidine chromogen, and color intensity was adjusted under the microscope. Finally, sections were counterstained, differentiated, dehydrated, and mounted, followed by quantification using Image-Pro Plus software.

### Real-time PCR

Total RNA was extracted from hepatocytes using Trizol reagent, and 1 µg of total RNA was reverse-transcribed into cDNA under the following conditions: 37°C for 15 min, 85°C for 5 s, and 4°C for 10 min, and finally stored at -20°C. The reverse transcription products were subjected to real-time PCR using β-actin as internal reference in a 10-µL reaction under the following amplification conditions: 95°C for 30 s, followed by 40 cycles of 95°C for 5 s, 55°C for 30 s, and 72°C for 30 s. Melting curve: 95°C for 0 s, 65°C for 15 s, and 95°C for 0 s. The primers used are listed in Table 1.

### Western blotting

Total protein was extracted from frozen liver tissues using RIPA Lysis Buffer and quantified by the bicinchoninic acid assay method. Equal amounts of protein from each group were subjected to SDS-PAGE and Western blotting. Proteins were transferred onto a PVDF membrane, which was then immersed into 5% skimmed milk for blocking and rinsed with Tris-buffered saline with Tween-20 (TBST). An anti-β-actin antibody (43 kDa) and primary antibodies against IL-1β, IL-6, TNFα, and NF-κB p65 were diluted in primary antibody dilution buffer and reacted overnight with the membrane at 4°C. After the reaction, the membrane was rinsed with TBST and then incubated with horseradish peroxidase-conjugated secondary antibody at

room temperature with agitation, followed by enhanced chemiluminescence development. The grayscale intensity of target protein bands was measured using ImageJ software (NIH, USA) with β-actin as internal reference. The intensity ratio of target protein to internal reference represents the relative expression level of target proteins.

### Serological testing

Determination of serum LPL levels was performed by enzyme-linked immunosorbent assay (ELISA). The standards were diluted prior to the assay. Both samples and standards were added into each well of the plate, which was then incubated at 37°C, rinsed, and incubated again following addition of enzyme-labeled reagent. Next, each well was rinsed and chromogen A and B solutions were added for color development at 37°C, followed by addition of stop solution. The plates were then evaluated within 15 min of stopping the reaction.

TG and TC levels were determined by the peroxidase anti-peroxidase method in accordance with the manufacturer's instructions (Jiancheng Bioengineering Institute, China).

### Statistical analysis

Statistical analyses were carried out using SPSS 17.0 software (IBM, Armonk, NY, USA). Each experiment was repeated 3 times. All data in were obtained by a blind observer. The variable of each group is expressed as mean ± standard deviation. The normal distribution test was first performed and scores that conformed to a normal distribution were then subjected to multiple comparisons by one-way ANOVA. The between-group comparison was carried out using LSD-t method. P<0.05 denotes statistical significance.

## Results

### Body weight variation in the different animal groups

No statistically significant difference was detected between initial body weights (g) of animals from the 4 groups (P>0.05)

**Table 2.** Initial and final body weight, LPL, and blood lipid levels of rats in each group (mean  $\pm$  standard deviation).

Group	Number	Initial body weight (g)	Final body weight (g)	LPL ( $\mu$ g/L)	TG (mmol/L)	TC (mmol/L)
Control	15	231.2 $\pm$ 4.9	388.6 $\pm$ 21.0	0.46 $\pm$ 0.076	0.68 $\pm$ 0.072	1.71 $\pm$ 0.201
CIH	15	228.9 $\pm$ 4.5 <sup>a#</sup>	485.7 $\pm$ 41.3 <sup>a*</sup>	0.24 $\pm$ 0.065 <sup>a*</sup>	1.34 $\pm$ 0.173 <sup>a*</sup>	2.43 $\pm$ 0.347 <sup>a*</sup>
CIH+NS	15	229.3 $\pm$ 4.3 <sup>b#</sup>	488.1 $\pm$ 25.3 <sup>b#</sup>	0.23 $\pm$ 0.059 <sup>b#</sup>	1.37 $\pm$ 0.145 <sup>b#</sup>	2.43 $\pm$ 0.265 <sup>b#</sup>
CIH+NAC	15	230.5 $\pm$ 5.0 <sup>c#</sup>	401.6 $\pm$ 30.6 <sup>c*</sup>	0.61 $\pm$ 0.116 <sup>c*</sup>	0.84 $\pm$ 0.149 <sup>c*</sup>	1.78 $\pm$ 0.236 <sup>c*</sup>
F		0.367	45.771	45.665	45.932	33.298
P		0.671	<0.001	<0.001	<0.001	<0.001

Between-group comparisons: a, Control vs. CIH; b, CIH vs. CIH+NS; c, CIH+NS vs. CIH+NAC; \* statistically significant ( $P < 0.05$ ); # not statistically significant ( $P > 0.05$ ). Control – normoxic control; CIH – CIH model; CIH+NS – CIH+0.9% NaCl model control; CIH+NAC – CIH+N-acetylcysteine treatment.

(Table 2). However, statistically significant differences were observed in final body weight between groups CON and CIH and groups CIH+NS and CIH+NAC ( $P < 0.05$ ). In contrast, no statistically significant difference was observed in final body weight between groups CIH and CIH+NS ( $P > 0.05$ ). Rats in the CIH group showed a more significant body weight gain than those in the CON group, whereas the body weight of rats in the CIH+NAC group increased less significantly than that in the CIH+NS group, indicating that NAC exhibits a therapeutic effect.

#### Determination of histomorphological changes in the liver

Based on HE staining, lipid accumulation and vacuolization leading to hepatocellular fatty degeneration could be seen in liver sections from rats in groups CIH and CIH+NS, but not in the CON group (Figure 1A).

In lipid Oil Red “O” staining, red particles correspond to lipid-like material. The hepatocyte lipids in groups CIH and CIH+NS were clearly stained in red, whereas those of the CIH+NAC group presented only weak staining. A comparison of lipid expression using Oil Red “O” showed statistically significant differences between groups CON and CIH and groups CIH+NS and CIH+NAC with respect to the integrated optic density (IOD)/area ( $P < 0.05$ ). No statistically significant difference was observed between groups CIH and CIH+NS ( $P > 0.05$ ; Figure 1A, 1B).

Ultrastructural characteristics were viewed by TEM. Clustered lipid droplets, a large amount of autophagosomes and lysosomes, focal accumulation of glycogen in the rough endoplasmic reticulum, and sparse microvilli in the bile canaliculi were observed in liver sections from rats in groups CIH and CIH+NS. In contrast, these characteristics were rarely seen in sections from groups CON and CIH+NAC, indicating that drug treatment was effective (Figure 1A).

#### Determination of oxidative stress levels in hepatocytes

Significantly higher levels of ROS were detected in hepatocytes from rats in groups CIH and CIH+NS, and lower levels in group CIH+NAC. Differences in IOD/area between groups CON and CIH and groups CIH+NS and CIH+NAC were statistically significant ( $P < 0.05$ ), whereas no such difference was observed between groups CIH and CIH+NS ( $P > 0.05$ ; Figure 2).

#### Determination of inflammation levels in the liver

IL-1 $\beta$ , IL-6, and TNF $\alpha$  levels were significantly higher in groups CIH and CIH+NS, but lower in groups CON and CIH+NAC. Statistically significant differences were observed between groups CON and CIH and groups CIH+NS and CIH+NAC with respect to the IOD/area value of protein expression ( $P < 0.05$ ), whereas no statistically significant difference was observed between groups CIH and CIH+NS ( $P > 0.05$ ; Figure 3).

#### Determination of NF- $\kappa$ B p65, IL-1 $\beta$ , IL-6, and TNF $\alpha$ mRNA and protein levels in the liver

Real-time PCR showed significantly higher levels of NF- $\kappa$ B, IL-1 $\beta$ , IL-6, and TNF $\alpha$  mRNAs in groups CIH and CIH+NS, and lower levels in groups CON and CIH+NAC. Statistically significant differences in mRNA levels were detected between groups CON and CIH and groups CIH+NS and CIH+NAC ( $P < 0.05$ ), whereas no statistically significant difference was observed between groups CIH and CIH+NS ( $P > 0.05$ ; Figure 4A).

Comparison of relative levels of NF- $\kappa$ B, IL-1 $\beta$ , IL-6, and TNF $\alpha$  via Western blotting showed that these proteins were significantly more abundant in groups CIH and CIH+NS, and less so in groups CON and CIH+NAC. Statistically significant differences in relative protein levels were observed between groups CON and CIH and groups CIH+NS and CIH+NAC ( $P < 0.05$ ), whereas



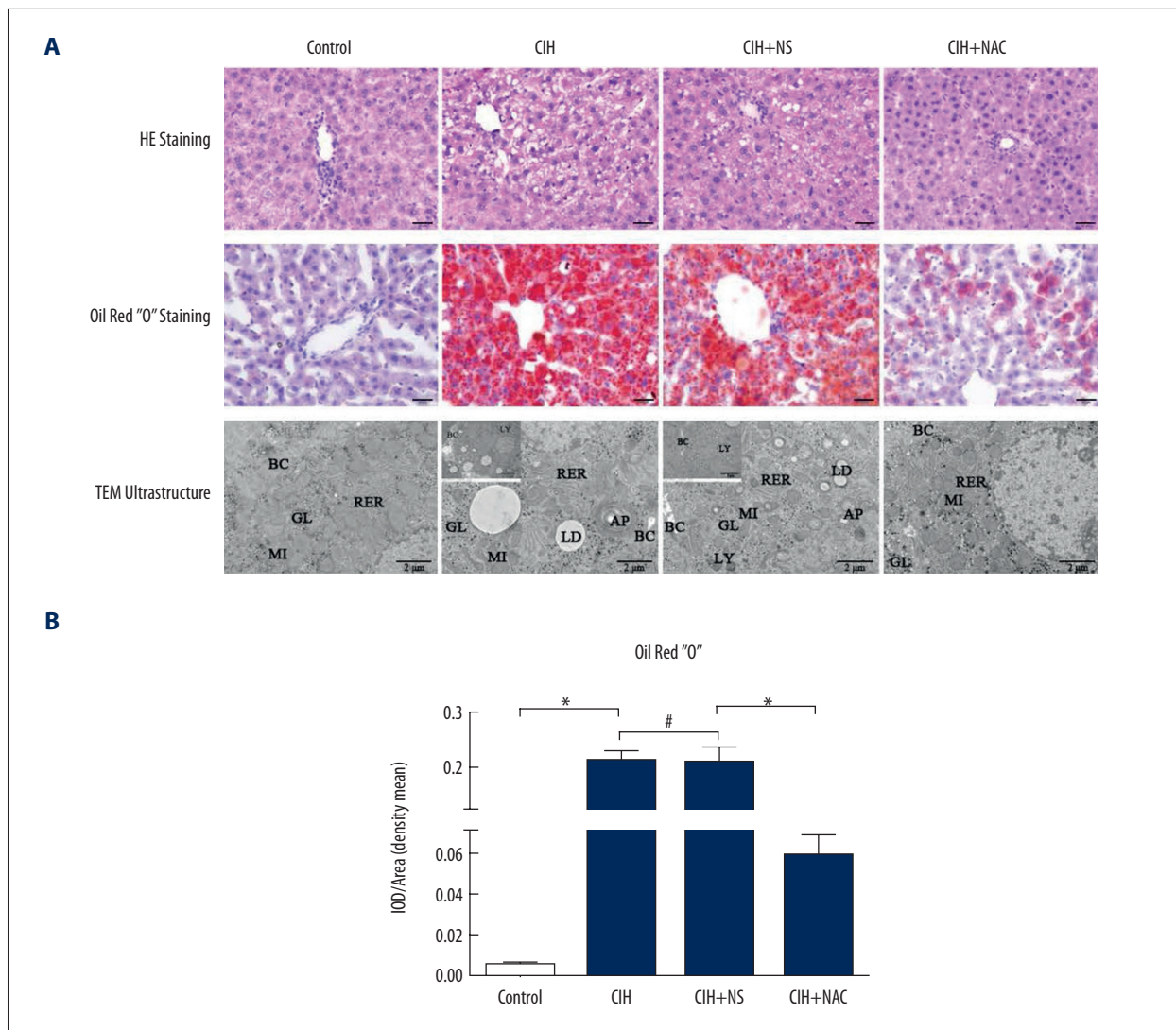


**Figure 1.** Qualitative and quantitative morphological changes in hepatocytes from 4 different rat groups: normoxic control (Control), chronic intermittent hypoxia model (CIH), CIH+0.9% NaCl model control (CIH+NS), and CIH+N-acetylcysteine treatment (CIH+NAC). **(A)** Hematoxylin and eosin (HE) and Oil Red "O" staining, scale bar: 20  $\mu$ m. Transmission electron microscopy (TEM), scale bar: 2  $\mu$ m (insets show a lower magnification, scale bar: 5  $\mu$ m). LD – lipid droplets; AP – autophagosomes; LY – lysosomes; BC – bile canaliculus; MI – mitochondria; RER – rough endoplasmic reticulum; GL – glycogen. **(B)** Integrated optical density (IOD)/area showing the mean value of cumulative Oil Red "O" optical density within the statistically effective area. \*  $P < 0.05$ ; #  $P > 0.05$ .

no statistically significant difference was observed between groups CIH and CIH+NS ( $P > 0.05$ ; Figure 4B).

#### Determination of serum LPL and blood TG and TC levels

Statistically significant differences were observed in serum LPL and blood lipid (TG and TC) levels between groups CON and CIH and groups CIH+NS and CIH+NAC ( $P < 0.05$ ), whereas no statistically significant difference was detected between groups CIH and CIH+NS ( $P > 0.05$ ). TG and TC blood levels increased but

serum LPL levels decreased in the CIH group, with the opposite tendencies in the CIH+NAC group ( $P < 0.05$ ; Table 2).

#### Discussion

The pathogenesis of CIH-induced liver injury in OSA patients is diverse and remains unclear [11]. CIH can activate the NF- $\kappa$ B signal transduction pathway in hepatocytes and other tissues, leading to inflammatory responses [12,13]; however, no specific, inner correlation with respect to its involvement

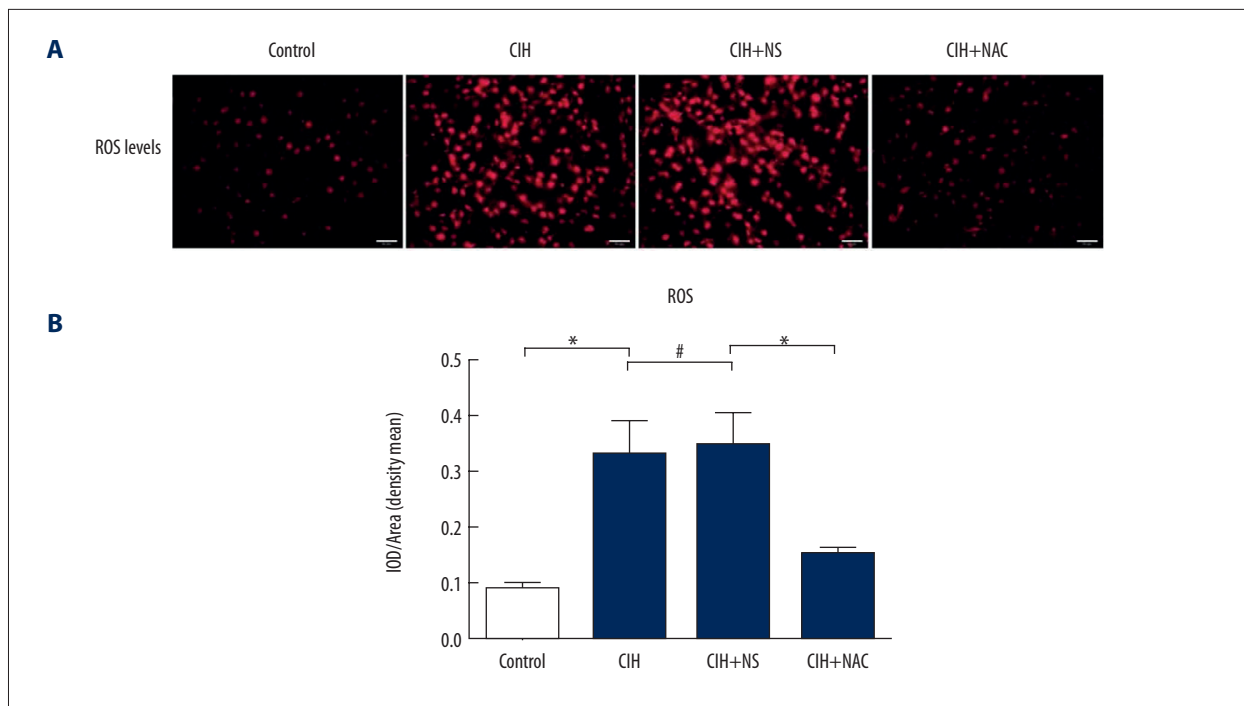


**Figure 2.** Levels of reactive oxygen species (ROS) in hepatocytes from 4 different rat groups: normoxic control (Control), chronic intermittent hypoxia model (CIH), CIH+0.9% NaCl model control (CIH+NS), and CIH+N-acetylcysteine treatment (CIH+NAC). **(A)** Red fluorescence indicates positive staining for ROS, scale bar: 20  $\mu\text{m}$ . **(B)** Integrated optical density (IOD)/area showing the mean value of cumulative ROS-positive optical density within the statistically effective area. \*  $P < 0.05$ ; #  $P > 0.05$ .

was observed so far. In addition, CIH mediates and regulates the inflammatory response via the HIF-1-SREBP-1-TG pathway [14,15]. Drager and Yao suggested that CIH-induced hypoxia inducible factor-1 inhibited LPL by upregulating the activity of angiopoietin like 4, thereby enhancing TG clearance in the plasma and TG intake in adipose tissue and internal organs, which may lead to tissue and organ injuries in OSA patients [16,17]. CIH also reduces the clearance of TG-rich lipoproteins in mice, thus inhibiting LPL activity in adipose tissue [18]. In the present study, morphological and cytokine level changes in rat liver tissue under CIH confirmed the presence of hepatocyte lipid accumulation and injury. Therefore, we infer that its possible pathogenesis is based on the elevated production of ROS in hepatocytes during metabolism under CIH, NF- $\kappa$ B translocation into the nucleus, and regulation of the levels of NF- $\kappa$ B signaling pathway components. Its over-activation greatly upregulates the expression of IL-1 $\beta$ , IL-6, and TNF $\alpha$ , which leads to downregulation of serum LPL levels and upregulation of TG and TC levels, thereby gradually resulting in liver damage. Lipid metabolism alteration or imbalance is an overreaction of hepatocytes to inflammation, which is an important factor leading to lipid accumulation in these cells. The pro-inflammatory signaling cascades are diverse and ROS/NF- $\kappa$ B signaling is a member of the family of pro-inflammatory signals. In addition, IL-1 $\beta$ , IL-6, and TNF $\alpha$  are important indicators of animal and human inflammatory responses and are also the

main factors that mediate injury to the body. When the body suffers some injury, including CIH-induced liver injury, the levels of cytokines like IL-1 $\beta$ , IL-6, and TNF $\alpha$  are increased. CIH has been reported to lead to hypercholesterolemia, lipid peroxidation, and inflammatory response; the degree of lipid metabolism alteration is associated with the severity of hypoxia [19]. CIH can lead to mild liver injury via lipid peroxidation in hepatocytes and over-accumulation of glycogen [20]. It has also been reported that CIH activates NF- $\kappa$ B in endothelial cells, which has been shown to regulate pro-inflammatory cytokines [21]. Substantial evidence suggests that CIH plays an important role in promoting cell apoptosis and can significantly increase the transcription activity of NF- $\kappa$ B, which can be activated under CIH/reoxygenation [22].

We found that most rats remained extremely still in the hypoxic environment and entered the “sleep in an abnormal position” state, which became increasingly frequent over time. They only recovered to an active status after the end of the hypoxic session and return to a normal environment. Rats showed an abnormal body weight gain under hypoxia and returned to a normal weight gain after treatment with NAC ( $P < 0.05$ , Table 2), indicating that the animals are more prone to obesity under a hypoxic environment. This phenomenon can be attributed to an increased accumulation and intake of lipids due to inflammation in various organs and tissues, including

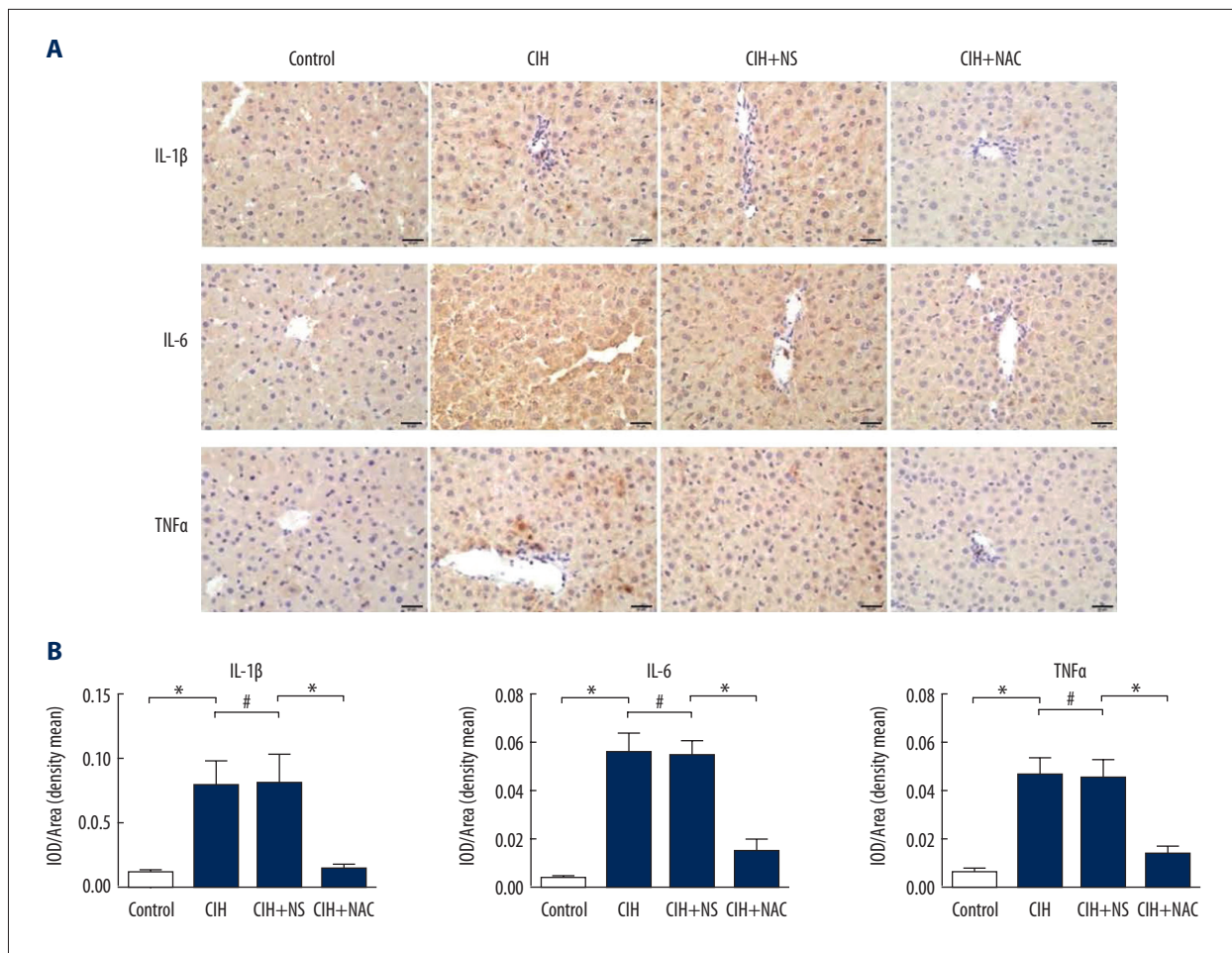


**Figure 3.** Levels of inflammatory cytokines in rat liver tissue determined using immunohistochemical staining in 4 different rat groups: normoxic control (Control), chronic intermittent hypoxia model (CIH), CIH+0.9% NaCl model control (CIH+NS), and CIH+N-acetylcysteine treatment (CIH+NAC). (A) Brownish yellow particles indicate positive expression, scale bar: 20  $\mu$ m. IL – interleukin; TNF $\alpha$  – tumor necrosis factor alpha. (B) Integrated optic density IOD/area showing the mean value of cumulative immunohistochemistry-positive optical density within the statistically effective area. \* P<0.05; # P>0.05.

the liver; alternatively, it might also be due to reduced activity and energy consumption. Obesity complicated by OSA has a high prevalence [23], although studies on the mechanism of obesity and OSA are relatively rare. St-Onge and Shechter suggested that frequent short sleep duration was the main manifestation in OSA patients due to frequent intermittent hypoxia that reduced sleep quality, leading to energy imbalance in the body and weight gain [24]. Recently, Olea et al. studied CIH and obesity-related blood glucose, insulin indicators, sympathetic nervous system activity, and arterial pressure, and discussed the results from different perspectives [25].

Recent studies on the protective effect of NAC focused mainly on the respiratory, cardiovascular, and central nervous system aspects. In our experiments, rat liver tissue in the CIH+NAC group was evaluated with respect to both cell morphology and molecular indicators. We propose that NAC causes a reduction

in ROS levels and inhibition of the ROS/NF- $\kappa$ B signaling pathway, alleviating inflammation and attenuating alterations in lipid metabolism. Results also indicate that NAC may play a role in improving CIH-induced liver tissue oxidative injury in rats, but its protective effect on OSA patients remains to be studied.

Our study shows that rat liver tissue generates ROS via oxidative stress under CIH, triggers the activation of the NF- $\kappa$ B signaling pathway possibly, regulates the expression of IL-1 $\beta$ , IL-6, and TNF $\alpha$ , as well as upregulates serum TG and TC levels, and downregulates serum LPL levels. These changes gradually result in hepatic lipid metabolism alterations and abnormal body weight gain. In addition, our study also confirmed the effectiveness of the experimental drug NAC. NAC can attenuate lipid metabolism alterations and abnormal weight gain in the CIH rat model; its mechanism of action may be related to inhibition of the ROS/NF- $\kappa$ B signaling pathway.

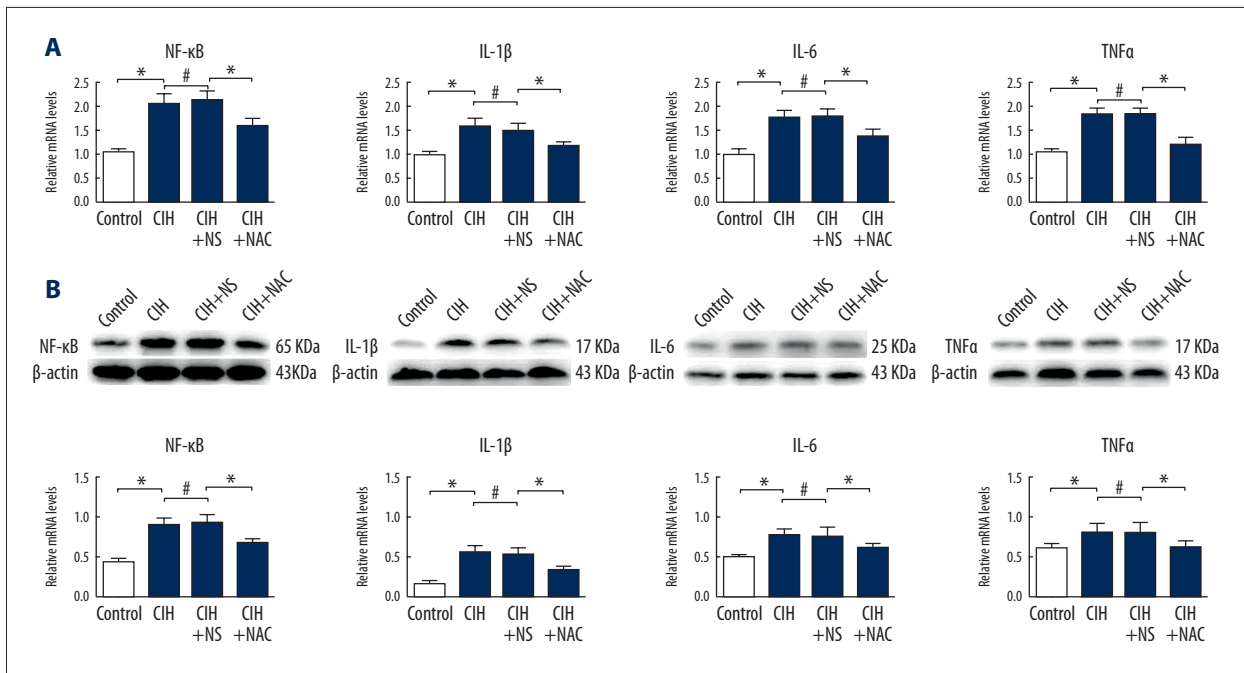


**Figure 4.** Protein and mRNA expression levels of nuclear factor-kappa B (NF-κB) and inflammatory cytokines in liver tissues from 4 rat groups: normoxic control (Control), chronic intermittent hypoxia model (CIH), CIH+0.9% NaCl model control (CIH+NS), and CIH+N-acetylcysteine treatment (CIH+NAC). **(A)** Determination of gene expression levels by real-time PCR. \*  $P < 0.05$ ; #  $P > 0.05$ . **(B)** Determination of protein levels by Western blotting. IL – interleukin; TNFα – tumor necrosis factor alpha. \*  $P < 0.05$ ; #  $P > 0.05$ .

## Conclusions

The harmful effects of CIH on rat liver are possibly associated with the reactive oxygen species (ROS)/NF-κB signaling pathway. NAC is capable of attenuating lipid metabolism alterations and abnormal body weight gain in the CIH rat model, via a possible mechanism related to inhibition of ROS/NF-κB signaling.

## References:

- Sabato R, Guido P, Salerno FG et al: Airway inflammation in patients affected by obstructive sleep apnea. *Monaldi Arch Chest Dis*, 2006; 65: 102–5
- Sookoian S, Pirola CJ: Obstructive sleep apnea is associated with fatty liver and abnormal liver enzymes: A meta-analysis. *Obes Surg*, 2013; 23: 1815–25
- Gharib SA, Khalyfa A, Abdelkarim A et al: Intermittent hypoxia activates temporally coordinated transcriptional programs in visceral adipose tissue. *J Mol Med (Berl)*, 2012; 90: 435–45
- Tanne F, Gagnadoux F, Chazouilleres O et al: Chronic liver injury during obstructive sleep apnea. *Hepatology*, 2005; 41: 1290–96
- Musso G, Cassader M, Olivetti C et al: Association of obstructive sleep apnea with the presence and severity of non-alcoholic fatty liver disease: A systematic review and meta-analysis. *Obes Rev*, 2013; 14: 417–31
- Toyama Y, Chin K, Chihara Y et al: Association between sleep apnea, sleep duration, and serum lipid profile in an urban, male, working population in Japan. *Chest*, 2013; 143: 720–28
- Wang H, Tian JL, Feng SZ et al: The organ specificity in pathological damage of chronic intermittent hypoxia: An experimental study on rat with high-fat diet. *Sleep Breath*, 2013; 17: 957–65
- Briancon-Marjollet A, Monneret D, Henri M et al: Endothelin regulates intermittent hypoxia-induced lipolytic remodelling of adipose tissue and phosphorylation of hormone-sensitive lipase. *J Physiol*, 2016; 594: 1727–40
- Shortt CM, Fredsted A, Chow HB et al: Reactive oxygen species mediated diaphragm fatigue in a rat model of chronic intermittent hypoxia. *Exp Physiol*, 2014; 99: 688–700
- da Rosa DP, Forgiarini LF, de Silva MB et al: Antioxidants inhibit the inflammatory and apoptotic processes in an intermittent hypoxia model of sleep apnea. *Inflamm Res*, 2015; 64: 21–29
- Zhen YQ, Wu YM, Sang YH et al: 2,3-Oxidosqualene cyclase protects liver cells from the injury of intermittent hypoxia by regulating lipid metabolism. *Sleep Breath*, 2015; 19: 1475–81
- Burioka N, Koyanagi S, Fukuoka Y et al: Influence of intermittent hypoxia on the signal transduction pathways to inflammatory response and circadian clock regulation. *Life Sci*, 2009; 85: 372–78
- Quintero M, Gonzalez-Martin MC, Vega-Agapito V et al: The effects of intermittent hypoxia on redox status, NF-κB activation, and plasma lipid levels are dependent on the lowest oxygen saturation. *Free Radical Biol Med*, 2013; 65: 1143–54

## Acknowledgements

We thank D. Xin-ran Cao and the WeiYa Center of Electron Microscopy for expert technical assistance.

## Conflict of interest

None.



14. Li J, Bosch-Marce M, Nanayakkara A et al: Altered metabolic responses to intermittent hypoxia in mice with partial deficiency of hypoxia-inducible factor-1alpha. *Physiol Genomics*, 2006; 25: 450–57
15. Siques P, Brito J, Naveas N et al: Plasma and liver lipid profiles in rats exposed to chronic hypobaric hypoxia: Changes in metabolic pathways. *High Alt Med Biol*, 2014; 15: 388–95
16. Yao Q, Shin MK, Jun JC et al: Effect of chronic intermittent hypoxia on triglyceride uptake in different tissues. *J Lipid Res*, 2013; 54: 1058–65
17. Drager LF, Yao Q, Hernandez KL et al: Chronic intermittent hypoxia induces atherosclerosis via activation of adipose angiopoietin-like 4. *Am J Respir Crit Care Med*, 2013; 188: 240–48
18. Drager LF, Li J, Shin MK et al: Intermittent hypoxia inhibits clearance of triglyceride-rich lipoproteins and inactivates adipose lipoprotein in a mouse model of sleep apnoea. *Eur Heart J*, 2012; 33: 783–90
19. Li J, Savransky V, Nanayakkara A et al: Hyperlipidemia and lipid peroxidation are dependent on the severity of chronic intermittent hypoxia. *J Appl Physiol*, 2007; 102: 557–63
20. Savransky V, Nanayakkara A, Vivero A et al: Chronic intermittent hypoxia predisposes to liver injury. *Hepatology*, 2007; 45: 1007–13
21. Li D, Wang C, Li N, Zhang L: Propofol selectively inhibits nuclear factor-κB activity by suppressing p38 mitogen-activated protein kinase signaling in human EA.hy926 endothelial cells during intermittent hypoxia/reoxygenation. *Mol Med Rep*, 2014; 9: 1460–66
22. Toffoli S, Roegiers A, Feron O et al: Intermittent hypoxia is an angiogenic inducer for endothelial cells: Role of HIF-1. *Angiogenesis*, 2009; 12: 47–67
23. Briancon-Marjollet A, Monneret D, Henri M et al: Intermittent hypoxia in obese Zucker rats: Cardiometabolic and inflammatory effects. *Exp Physiol*, 2016; 101: 1432–42
24. St-Onge MP, Shechter A: Sleep disturbances, body fat distribution, food intake and/or energy expenditure: Pathophysiological aspects. *Horm Mol Biol Clin Investig*, 2014; 17: 29–37
25. Olea E, Agapito MT, Gallego-Martin T et al: Intermittent hypoxia and diet-induced obesity: Effects on oxidative status, sympathetic tone, plasma glucose and insulin levels, and arterial pressure. *J Appl Physiol*, 2014; 117: 706–19